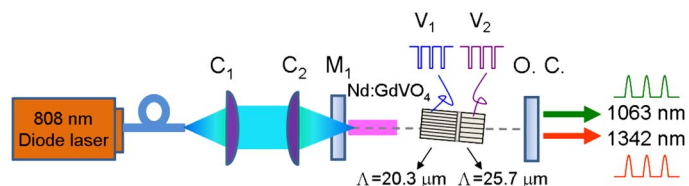


Selectable Dual-Wavelength Actively Q-Switched Laser by Monolithic Electro-Optic Periodically Poled Lithium Niobate Bragg Modulator

Volume 5, Number 5, October 2013

Shou-Tai Lin
Shang-Yu Hsu
Yen-Yin Lin
Yuan-Yao Lin



DOI: 10.1109/JPHOT.2013.2280347
1943-0655 © 2013 IEEE

Selectable Dual-Wavelength Actively Q-Switched Laser by Monolithic Electro-Optic Periodically Poled Lithium Niobate Bragg Modulator

Shou-Tai Lin,¹ Shang-Yu Hsu,¹ Yen-Yin Lin,² and Yuan-Yao Lin²

¹Department of Photonics, Feng Chia University, Taichung 40724, Taiwan

²Institute of Photonics Technologies, National Tsing Hua University, Hsinchu 30013, Taiwan

DOI: 10.1109/JPHOT.2013.2280347
1943-0655 © 2013 IEEE

Manuscript received June 3, 2013; revised August 20, 2013; accepted August 20, 2013. Date of publication August 30, 2013; date of current version September 6, 2013. This work was supported by the National Science Council of Taiwan under Contracts NSC 100-2221-E-035-063-MY3 and NSC 101-2221-E-007-105. Corresponding author: S.-T. Lin (e-mail: stailin@fcu.edu.tw).

Abstract: A novel dual-wavelength actively Q-switched laser by a cascaded electrooptic periodically poled lithium niobate (PPLN) Bragg modulator has been developed. Two PPLN Bragg modulators with grating period $\Lambda_1 = 20.3$ (EPBM1) and $\Lambda_2 = 25.7 \mu\text{m}$ (EPBM2) are integrated monolithically and used to separately Q-switch the transitions between $^4\text{F}_{3/2} \rightarrow ^4\text{I}_{11/2}$ and $^4\text{F}_{3/2} \rightarrow ^4\text{I}_{13/2}$ at the same Bragg angle. When applying 20-W diode power and 1-kHz Q-switching rate, the output wavelength can be selected between 1063 and 1342 nm with the peak power values of 27.6 and 1.6 kW, respectively. Utilizing two LBO crystals and an intracavity frequency doubling configuration, the green and red lasers can be selectively generated with the peak power values of 19 and 0.183 kW, respectively. The coupling effect between two PPLN Bragg modulators can be further reduced by adopting a longer EPBM1 and enhancing the performance of $^4\text{F}_{3/2} \rightarrow ^4\text{I}_{13/2}$ at the high pump power region.

Index Terms: Diode-pumped lasers, Q-switched lasers.

1. Introduction

Diode-pumped, Q-switched Nd-laser systems of $^4\text{F}_{3/2} \rightarrow ^4\text{I}_{11/2}$ ($1 \mu\text{m}$), and $^4\text{F}_{3/2} \rightarrow ^4\text{I}_{13/2}$ ($1.3 \mu\text{m}$) have been extensively studied due to its high conversion efficiency and numerous applications in material processing, optical communication as well as medical treatment. Through optical parametric process, the wavelength can be further extended to mid-IR or THz region which is useful in spectroscopy and environmental sensing. Frequency doubling to the green and red color is also attractive for entertainment and microscopy. However, the emission cross section differences between two transitions increase the difficulty to manipulate two wavelengths simultaneously [1]. Employing separate cavities and varied spatial overlapping between pump and resonated waves, a dual-wavelength system can be produced with balanced output power [2], [3]. Another dual-wavelength scheme appeared in different time sequence was also proposed by using two active loss modulators with an adjustable delay time [4], [5]. However, a separate cavity increased the cavity length and generated a moderate pulse width which produced the lower peak power. Adopting single or double saturable absorbers was also proposed to generate dual-wavelength Q-switch pulse [6], [7]. The inherent instability of saturable absorber increases the complexity and limits the application. Recently, Lin *et al.* [8] reported a cw triple-wavelength selectable Nd-laser by electro-optic periodically

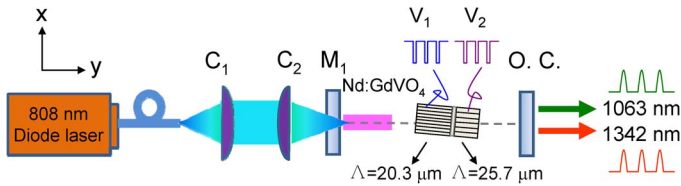


Fig. 1. Schematic of the dual-wavelength switchable Nd:GdVO₄ laser pumped by a 808 nm diode laser. The EPBM functions as a Q-switcher or electro-optic loss modulator controlled by the applied voltage and the separate electrode can individually modulate 1063 and 1342 nm at the same Bragg angle.

poled lithium niobate Bragg modulators (EPBM). The gain competitions among 0.9, 1 and 1.3 μm waves were controlled through actively manipulating the loss of 1 and 1.3 μm by dc voltages applied to a monolithic EPBM. When an electric field is applied on the Z-axis of EPBM, the positive and negative domains experience different index changed while their optical axes still keep the same. Once a laser matches the Bragg incident angle $\theta_{B,m} = \sin^{-1}(m\lambda_0/(2n\Lambda))$, the deflection efficiency is a function of laser beam radius and applied voltage [9], [10], where m is the diffraction order, λ_0 is the laser wavelength, n is the average refractive index of the grating, and Λ is the grating period. Through a lithographic define of grating period and standard high-voltage poling process [11], the cascaded Bragg modulators provide the possibility to modulate separate wavelengths in a single device. Since the pulsed laser has a high peak power and suitable for practical applications, a dual-wavelength Q-switched laser was developed. In this report, we present a simple linear cavity to modulate the loss of $^4F_{3/2} \rightarrow ^4I_{11/2}$, and $^4F_{3/2} \rightarrow ^4I_{13/2}$ as well as Q-switch two wavelengths separately by a cascaded EPBM. Hence we are able to show in the following a novel configuration of dual-wavelength Q-switched Nd-laser between 1 and 1.3 μm .

2. Experimental Setup

Fig. 1 shows an experimental configuration of dual-wavelength Q-switched laser via EPBM in a diode-pumped Nd:GdVO₄ laser. A 20 W fiber-pigtailed diode laser at 808 nm was adopted to pump an a-cut, 5 mm long, 0.4-at.% Nd-doped GdVO₄ crystal through a set of 1 to 3 coupling lenses. The core diameter of the fiber was 200 μm . To dissipate the heat generation, the Nd:GdVO₄ crystal was wrapped by indium foil and kept in a copper block for water cooling at 18 °C. The input surfaces of the Nd:GdVO₄ crystal were optically polished and coated with anti-reflection coating ($R < 1\%$) at 808, 1063 and 1342 nm. The linear laser cavity was constructed by a flat high reflection (HR) ($R > 99.8\%$) coated mirror M_1 and flat output coupler with 35 and 7% output coupling at 1063 and 1342 nm, respectively. The periodically poled lithium niobate (PPLN) crystal was a 5 mol.% MgO doped PPLN (made by HC Photonics, Taiwan). The dimensions of PPLN are 10 mm (length in x) \times 15.5 mm (width in y) \times 2 mm (thickness in z) and are separated in two sections, EPBM1 and EPBM2, for diffracting 1063 and 1342 nm at the same Bragg angle $\theta_{B,1}(1063 \text{ nm}) = \theta_{B,2}(1342 \text{ nm}) = 0.7^\circ$. The grating period of EPBM1 is 20.3 μm and the dimensions are 10 mm (length in x) \times 9 mm (width in y). The grating period of EPBM2 is 25.74 μm and the dimensions are 10 mm (length in x) \times 6 mm (width in y). The half-wave voltages of 20.3 and 25.74 μm gratings were measured at 660 and 940 V, respectively. The end surfaces of the EPBM were optically polished and had anti-reflection coating at 1063 and 1342 nm ($R < 1\%$). To independently apply the electric field, two separate NiCr electrodes were coated on $\pm z$ surfaces of EPBM1 and EPBM2. The total cavity length was around 100 mm. When varied the thermal focal length of Nd:GdVO₄ crystal at the whole pump power range, the beam radius inside the EPBM was calculated between 200 to 250 μm at 1063 nm which contributed more than 50% loss modulation at the half-wave voltage [9]. The polarization of the Nd:GdVO₄ was align to the z-axis of EPBM to utilize larger γ_{33} Pockels coefficient. A dichroic coated mirror was used to separate 1063 and 1342 nm and a pyroelectric detector was adopted to record the pulse energy. To record the temporal characteristic, a fast InGaAs detector (rise time < 175 ps) and a 1 GHz bandwidth oscilloscope were used.

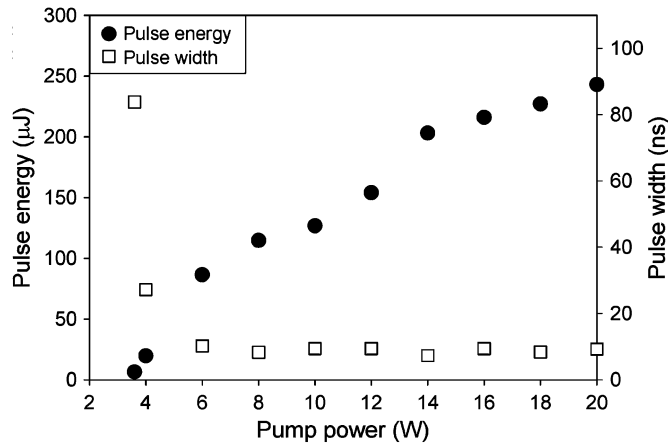


Fig. 2. Measured 1063 nm pulse energy and pulse width versus diode power. The filled and open dots denote the measured pulse energy and pulse width, respectively.

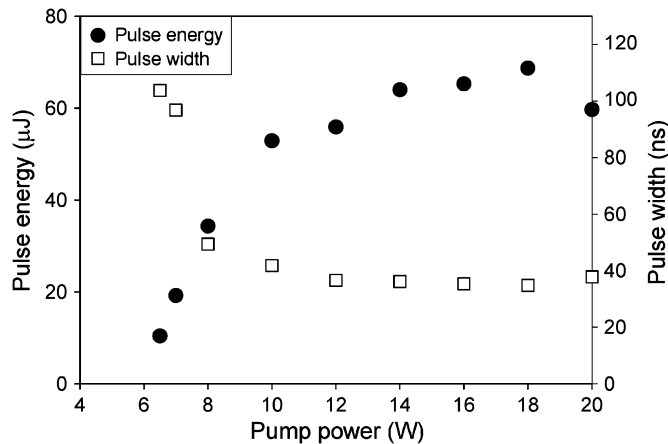


Fig. 3. Measured 1342 nm pulse energy and pulse width versus diode power. The filled and open dots denote the measured pulse energy and pulse width, respectively.

3. Experimental Result

Due to the stress-induced refractive index change in the MgO:PPLN [12], the zero-diffraction was measured at around -300 V. Without any biased voltage, more than 30% diffraction loss at 1063 nm was contributed by EPBM1 and EPBM2. To Q-switch 1063 nm, a negative pulsed voltage with 300 V, $1\ \mu\text{s}$ pulse width at 1 kHz repetition rate drove EPBM1 and EPBM2. Fig. 2 shows the measured pulse energy and pulse width versus diode power at 1063 nm. After overcoming the cavity threshold at 4.5 W, the pulse energy was increased monotonically. At the maximum diode power, the 1063 nm pulse has $270\ \mu\text{J}$ energy and 9.8 ns width, corresponding to a peak power of 27.6 kW. Although the wavelength of 1342 nm also matched the Bragg condition in the Q-switching process, none of 1342 nm was measured. During the gain competition, 1342 nm was completely suppressed. To Q-switch 1342 nm, the pulsed voltage was only applied to EPBM2. Without applying any voltage to EPBM1, the gain of 1063 nm was suppressed by the stress-induced diffraction loss when the diode power was below 18 W. After overcoming the cavity threshold around 6 W, the maximum pulse energy of 1342 nm was reached $69\ \mu\text{J}$ at 18 W diode power, as shown in Fig. 3. Due to the insufficient gain suppression of 1063 nm, the pulse energy of 1342 nm was decreased effectively at the diode power higher than 18 W. Dual-wavelength generation was observed when the pump power operated between 18 and 20 W.

To study the gain competition between 1063 and 1342 nm, a dc voltage was further applied to EPBM1 and the pulsed voltage only drove EPBM2. At 20 W diode power, a wavelength selectable

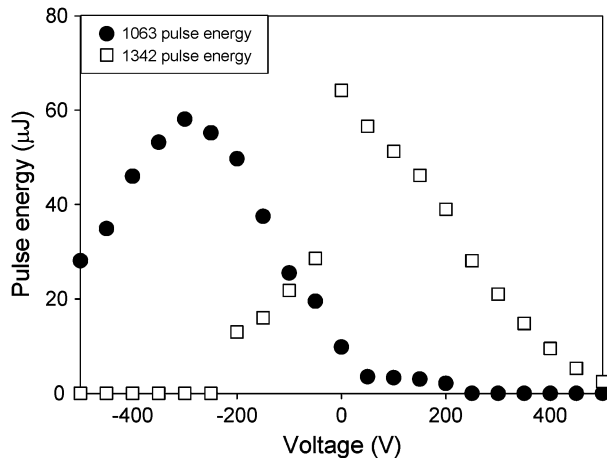


Fig. 4. Measured 1063 and 1342 nm pulse energy versus dc voltage of EPBM1 when the diode power was fixed at 20 W and the 1 kHz pulsed voltage was applied to EPBM2. The filled and open dots denote the measured pulse energy of 1063 and 1342 nm, respectively.

laser was realized by switching the dc voltage, as shown in Fig. 4. When the applied dc voltages were operated at ~ -300 and 50 V, a dual-wavelength Q-switched laser between 1063 and 1342 nm was generated. Although 1063 nm was not matched Bragg angle of EPBM2, the Q-switching process was still realized which caused by the broad acceptance bandwidth of EPBM2. The maximum pulse energy of 1063 nm was measured at dc voltage of -300 V where the stress-induced Bragg deflection was eliminated. Although none of 1063 nm was measured at the dc voltage higher than 200 V, the performance of 1342 nm was also affected by EPBM1. To reduce the coupling effect between EPBM1 and EPBM2, the increased crystal length of EPBM1 or slightly differed the incident Bragg angles by redesigning the grating periods is the possible method.

In order to produce a dual-wavelength laser in the visible region, the output coupler was replaced by another flat mirror which had high reflection coating ($R > 99\%$) at both 1063 and 1342 nm as well as high transmission ($T > 90\%$) at 532 and 671 nm. Two 10-mm-long LBO crystals (Green LBO: $\theta = 90^\circ$, $\varphi = 10.7^\circ$, Red LBO: $\theta = 85^\circ$, $\varphi = 0^\circ$) with phase-matching temperature at ~ 40 degree and type I phase matching were adopted for processing intracavity frequency doubling. The LBO crystals were placed in close to the output coupler for reaching the beam waist of resonated wave. To generate the green laser, the negative pulsed voltage at 1 kHz drove both EPBM. After overcoming the cavity threshold of 3 W, the green laser at 20 W diode power has $80 \mu\text{J}$ energy and 4.2 ns width, corresponding to a peak power of 19 kW. Due to the high conversion efficiency in the intracavity frequency doubling scheme, the pulse width of 531.5 nm was reduced to 4.2 ns, as shown in Fig. 5. To generate the red laser, the pulsed voltage only drove EPBM2 and a dc voltage with 300 V was applied to EPBM1 to suppress the gain of 1063 nm. After overcoming the cavity threshold of 8 W, the red laser at 20 W pump power has $5.2 \mu\text{J}$ energy and 28.4 ns width, corresponding to a peak power of 0.183 kW, as shown in Fig. 6.

4. Coupling Effect Analysis

To analyze the coupling effect between EPBM1 and EPBM2, coupled wave equations with assumptions of plane-wave, small incident angle and slowly varying-envelope were adopted [13], given by

$$\frac{dA_1}{dy} = i\kappa A_2 e^{-i\Delta ky} \quad \frac{dA_2}{dy} = i\kappa^* A_1 e^{i\Delta ky} \quad (1)$$

where A_1 and A_2 are the incident and diffracted electric field, respectively, $\kappa = k(\Delta n_e/2n_e)$ is the coupling coefficient, $n(x) = n_e + s(x)\Delta n_e$ and $\Delta n_e = (2/\pi)((1/2)n_e^3\gamma_{33}(V_z/d))$ are the induced refractive index change by Pockels effect, $s(x) = \pm 1$ denotes the sign of the domain orientation of the PPLN crystal, and Δk is the wave vector mismatched in the y direction. To simplify the analysis, only the

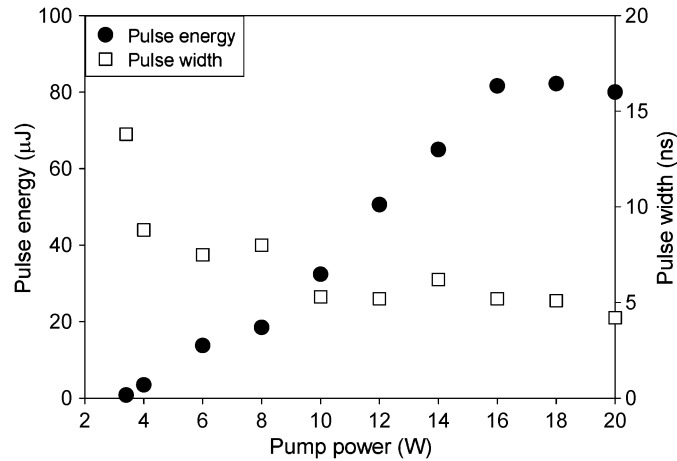


Fig. 5. Measured 531.5 nm pulse energy and pulse width versus diode pump power. The filled and open dots denote the measured pulse energy and pulse width, respectively.

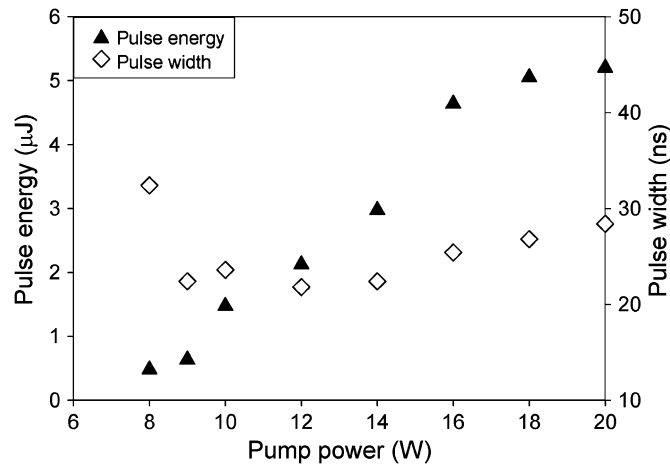


Fig. 6. Measured 671 nm pulse energy and pulse width versus diode pump power. The filled and open dots denote the measured pulse energy and pulse width, respectively.

TABLE 1

The parameters used in the calculation

Parameters	Value
PPLN grating period	20.3 μm
Incident angle	0.7 degree
PPLN thickness (d)	2 mm
PPLN length (L)	9 / 18 mm
Pockels coefficient	30 pm/V

first Fourier coefficient of the square index profile of PPLN is considered. The diffraction efficiency versus mismatched Δk is then derived to be [13]

$$\eta(\Delta k) = \frac{|A_2(L)|^2}{|A_1(0)|^2} = \frac{|\kappa|^2}{|\kappa|^2 + (\frac{1}{2}\Delta k)^2} \sin^2 \left\{ \left[|\kappa|^2 + \left(\frac{1}{2}\Delta k \right)^2 \right]^{1/2} L \right\}. \quad (2)$$

The detailed parameters used in the calculation are shown in Table 1. Fig. 7 shows the calculated Bragg diffraction efficiency versus applied voltage of EPBM1. The incident angle is kept at 0.7°. The black lines

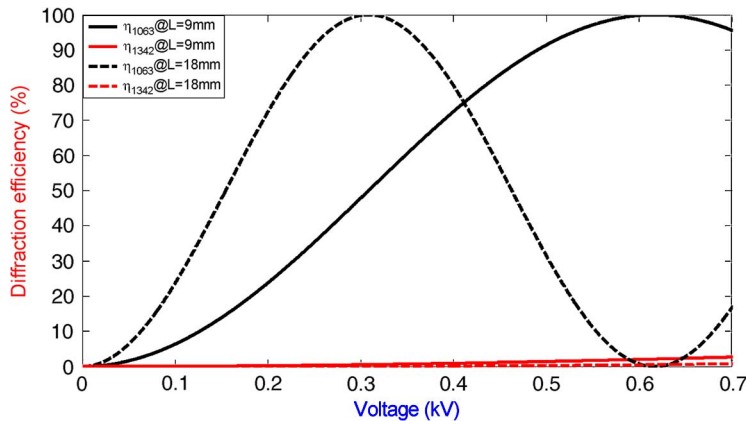


Fig. 7. Calculated Bragg diffraction efficiency of 1063 and 1342 nm at 9 and 18 mm PPLN lengths. The period of PPLN Bragg modulator is $20.3\text{ }\mu\text{m}$ and the incident angle is 0.7° phase-matched at 1063 nm.

show the phase-matched wavelength, 1063 nm and the half-wave voltages are calculated to be 620 and 310 V for 9 and 18 mm PPLN length, respectively. For mismatched wavelength, 1342 nm, the red lines show the diffraction loss at the half-wave voltage calculated to be 2.2 and 0.1% for 9 and 18 mm PPLN length, respectively. More than an order reduction of the coupling loss is found while doubling the PPLN length. The longer crystal was helpful to decrease the coupling coefficient and mismatched coupling diffraction as well as provided the independence of dual wavelength switching control. Although 1342 nm experiences the slight diffraction in this simplified model, the high order Fourier components of square index profile and Gaussian beam divergence effect will further enhance the coupling effect.

5. Conclusion

In conclusion, we have demonstrated a novel dual-wavelength Q-switched laser by integrating two electro-optic PPLN Bragg modulators in a monolithic chip. The output wavelength can be selected through controlling the applied voltage on EPBM sections. At 20 W diode power and 1 kHz Q-switching rate, the output wavelength can be chosen between 1063 and 1342 nm with the peak power of 27.6 and 1.6 kW, respectively. Under the intracavity frequency doubling scheme, we can generate green (531.5 nm) or red (671 nm) laser with the peak power of 19 and 0.183 kW, respectively. The calculation result shows the coupling effect can be diminished by increasing the length of EPBM1 which will be helpful to Q-switch two wavelengths individually and enhance the performance of $^4F_{3/2} \rightarrow ^4I_{13/2}$.

References

- [1] C. Czeranowsky, M. Schmidt, E. Heumann, G. Huber, S. Kutovoi, and Y. Zavartsev, “Continuous wave diode pumped intracavity doubled Nd:GdVO₄ laser with 840 mW output power at 456 nm,” *Opt. Commun.*, vol. 205, no. 4-6, pp. 361–365, May 2002.
- [2] Y. F. Chen, S. W. Tsai, S. C. Wang, Y. C. Huang, T. C. Lin, and B. C. Wong, “Efficient generation of continuous-wave yellow light by single-pass sum-frequency mixing of a diode-pumped Nd:YVO₄ dual-wavelength laser with periodically poled lithium niobate,” *Opt. Lett.*, vol. 27, no. 20, pp. 1809–1811, Mar. 2002.
- [3] Y. F. Chen, “CW dual-wavelength operation of a diode-end-pumped Nd:YVO₄ laser,” *Appl. Phys. B*, vol. 70, no. 4, pp. 475–478, Apr. 2000.
- [4] G. A. Henderson, “A computational model of a dual-wavelength solid state laser,” *J. App. Phys.*, vol. 68, no. 11, pp. 5451–5455, Dec. 1990.
- [5] X. W. Fan, J. L. He, H. T. Huang, and L. Xue, “An intermittent oscillation dual-wavelength diode-pumped Nd: YAG Laser,” *IEEE J. Quantum Electron.*, vol. 43, no. 10, pp. 884–888, Oct. 2007.
- [6] H. T. Huang, J. L. He, B. T. Zhang, K. J. Yang, C. H. Zuo, J. L. Xu, X. L. Dong, and S. Zhao, “Intermittent oscillation of 1064 nm and 1342 nm obtained in a diode-pumped doubly passively Q-switched Nd:YVO₄ laser,” *Appl. Phys. B*, vol. 96, no. 4, pp. 815–820, Sep. 2009.

- [7] J. L. Xu, H. T. Huang, J. L. He, J. F. Yang, B. T. Zhang, X. Q. Yang, and F. Q. Liu, "Dual-wavelength oscillation at 1064 and 1342 nm in a passively Q-switched Nd:YVO₄ laser with V³⁺:YAG as saturable absorber," *Appl. Phys. B*, vol. 103, no. 1, pp. 75–82, Apr. 2011.
- [8] S. T. Lin and C. S. Hsieh, "Triple-wavelength Nd-laser system by cascaded electro-optic periodically poled lithium niobate Bragg modulator," *Opt. Exp.*, vol. 20, no. 28, pp. 29659–29664, Dec. 2012.
- [9] S. T. Lin, G. W. Chang, Y. Y. Lin, Y. C. Huang, A. C. Chiang, and Y. H. Chen, "Monolithically integrated laser Bragg Q-switch and wavelength converter in a PPLN crystal," *Opt. Exp.*, vol. 15, no. 25, pp. 17093–17098, Dec. 2007.
- [10] Y. Y. Lin, S. T. Lin, G. W. Chang, A. C. Chiang, Y. C. Huang, and Y. H. Chen, "Electro-optic periodically poled lithium niobate Bragg modulator as a laser Q-switch," *Opt. Lett.*, vol. 32, no. 5, pp. 545–547, Mar. 2007.
- [11] L. E. Myers, R. C. Eckardt, M. M. Fejer, R. L. Byer, W. R. Bosenberg, and J. W. Pierce, "Quasi-phase-matched optical parametric oscillators in bulk periodically poled LiNbO₃," *J. Opt. Soc. Am. B*, vol. 12, no. 11, pp. 2102–2116, Nov. 1995.
- [12] Y. Chen, H. Zhan, and B. Zhou, "Refractive index modulation in periodically poled MgO-doped congruent LiNbO₃," *Appl. Phys. Lett.*, vol. 93, no. 22, pp. 222902-1–222902-3, Dec. 2008.
- [13] R. W. Boyd, *Nonlinear Optics*. New York, NY, USA: Elsevier, 2003, pp. 393–402.